

Effect of nanoparticles mean diameter on mixed convection heat transfer of a nanofluid in a horizontal tube

S. Mirmasoumi¹, A. Behzadmehr *

Mechanical Engineering Department, Zahedan, Iran

Received 2 August 2007; received in revised form 25 October 2007; accepted 27 November 2007

Available online 22 January 2008

Abstract

Fully developed mixed convection of a nanofluid (water/Al₂O₃) has been studied numerically. Two-phase mixture model has been used to investigate the effects of nanoparticles mean diameter on the flow parameters. The calculated results demonstrate that the convection heat transfer coefficient significantly increases with decreasing the nanoparticles mean diameter. However it does not significantly change the hydrodynamics parameters. Nanoparticles distribution at the tube cross section shows that the non-uniformity of the particles distribution augments when using larger nanoparticles and/or considering relatively high value of the Grashof numbers.
© 2007 Elsevier Inc. All rights reserved.

Keywords: Nanofluid; Two-phase model; Laminar mixed convection; Horizontal tube; Nanoparticles mean diameter

1. Introduction

In order to manage the growing demand from different industries, heat exchanger devices have to be small in size, light in weight and of high performance. Low thermal conductivity of conventional heat transfer fluids such as water, oil, and ethylene glycol mixture is a serious limitation in improving the performance and compactness of these engineering equipments. To overcome this disadvantage, there is a strong motivation to develop advanced heat transfer fluids with substantially higher thermal conductivity. An innovative way of improving the thermal conductivities of fluids is to suspend small solid particles in the fluid. Various types of powders such as metallic, non-metallic and polymeric particles can be added into fluids to form slurries. By improving the technology to make particles in nanometer dimensions, a new generation of solid-liquid mixture that is called nanofluid, was appeared (Choi, 1995). The nanofluid is a new kind of fluid containing small quantity of nano-sized particles (usually less than 100 nm) that are uni-

formly and stably suspended in a liquid. The dispersion of a small amount of solid nanoparticles in conventional fluids changes their thermal conductivity remarkably.

Some benefits of nanofluids that make them useful are: a tiny size, along with a large specific surface area, high effective thermal conductivity and high stability and less clogging and abrasion (Wen and Ding, 2004). Thermal conductivity of nanofluid has been measured with several nanoparticles volume fraction, material and dimension in several base fluids and all findings show that thermal conductivity of nanofluid is higher than the base fluids.

Lee et al. (1999) have demonstrated that oxide ceramic nanofluids consisting of CuO or Al₂O₃ nanoparticles in water or ethylene glycol exhibit enhanced thermal conductivity. For example, using Al₂O₃ particles having mean diameter of 13 nm at 4.3% volume fraction increase the thermal conductivity of water under stationary conditions by 30% (Masuda et al., 1993). On the other hand, larger particles with an average diameter of 40 nm led an increase of less than 10% (Lee et al., 1999). Furthermore, the effective thermal conductivity of metallic nanofluid increase by up to 40% for the nanofluid consisting of ethylene glycol containing approximately 0.3% volume Cu nanoparticles of mean diameter less than 10 nm (Estman et al., 2001).

* Corresponding author. Tel.: +98 541 2446251; fax: +98 541 2447092.

E-mail address: behzadmehr@hamoon.usb.ac.ir (A. Behzadmehr).

¹ Present address: Chabahar Maritime University, Chabahar, Iran.

Nomenclature

C_f	peripherally average skin friction coefficient
C_p	specific heat (J/kg K)
D	tube diameter (m)
d_p	nanoparticle diameter (nm)
d_f	molecular diameter of base fluid
E	energy (J/kg)
g	gravitational acceleration (m s ⁻²)
Gr	Grashof number ($= \frac{g\beta_{\text{eff}}q''D^4}{K_{\text{eff}}v_{\text{eff}}^2}$)
h	convection heat transfer coefficient ($= \frac{q''}{T_w - T_b}$ (W/m ² K))
K	thermal conductivity (W/m K)
K_b	Boltzmann constant ($= 1.3807 \times 10^{-23}$ J/K)
Nu	peripherally average Nusselt number ($= \frac{q''D}{k_{\text{eff}}(T_w - T_b)}$)
P	pressure (pa)
Pr	Prandtl number ($= \frac{\nu_{\text{eff}}}{\alpha_{\text{eff}}}$)
q''	uniform heat flux (W/m ²)
r	radial direction
r_0	tube radial (m)
Re	Reynolds number ($= \frac{\rho_{\text{m}}D}{\mu_{\text{eff}}}$)
Ri	Richardson number ($= GrRe^{-2}$)
T	temperature (K)

V	velocity (m s ⁻¹)
Z	axial direction

Greek letters

α	thermal diffusivity
β	volumetric expansion coefficient (K ⁻¹)
θ	angular coordinate
ϕ	volume fraction
Φ	arbitrary variables
μ	Dynamic viscosity (N s m ⁻²)
ν	kinematic viscosity ($= \frac{\mu_{\text{eff}}}{\rho_{\text{eff}}}$ (m ² s ⁻¹))
ρ	density (kg m ⁻³)

Subscripts

b	bulk
dr	drift
eff	effective
f	base fluid
k	summation index
m	mixture
0	inlet condition
p	particle
w	wall

Different concepts have been proposed to explain this enhancement in heat transfer. [Xuan and Li \(2000\)](#) and [Xuan and Roetzel \(2000\)](#) have identified two causes of improved heat transfer by nanofluids: the increased thermal dispersion due to the chaotic movement of nanoparticles that accelerates energy exchanges in the fluid and the enhanced thermal conductivity of nanofluid. On the other hand [Keblinski et al. \(2002\)](#) have studied four possible mechanisms that contribute to the increase in nanofluid heat transfer: Brownian motion of the particles, molecular-level layering of the liquid/particles interface, ballistic heat transfer in the nanoparticles and nanoparticles clustering. Similarly to [Wang et al. \(1999\)](#), they showed that the effects of the interface layering of liquid molecules and nanoparticles clustering could provide paths for rapid heat transfer. Numerous theoretical and experimental studies have been conducted to determine the effective thermal conductivity of nanofluids. However, studies show that the measured thermal conductivity of nanofluid is much larger than the theoretical predictions ([Choi et al., 2001](#); [Zhang et al., 2007](#)). Many attempts have been made to formulate efficient theoretical models for the prediction of the effective thermal conductivity ([Xue, 2003](#); [Xuan et al., 2003](#); [Jang and Choi, 2004](#); [Chon et al., 2005](#)). [Chon et al. \(2005\)](#) reported an experimental correlation for the thermal conductivity of Al₂O₃ as a function of nanoparticles size and fluid temperature. They showed that the Brownian motion of nanoparticles constitutes a key mechanism of the thermal conductivity enhancement

with increasing temperature and decreasing nanoparticles size.

As nanofluids are rather new, relatively few theoretical and experimental studies have been reported on convective heat transfer coefficient in confined flows. [Pak and Cho \(1998\)](#) and [Xuan and Li \(2000, 2003\)](#) obtained experimental results on convective heat transfer for laminar and turbulent flow of a nanofluid inside a tube. They produced the first empirical correlations for the Nusselt number using nanofluids composed of water and Cu, TiO₂ and Al₂O₃ nanoparticles. The results indicate a remarkable increase in heat transfer performance over the base fluid for the same Reynolds number.

Because of the fact that heat transfer occurs on the particle surface, it is expected that the nanofluids show better thermal property in comparison with conventional heat transfer fluids and also other fluids which consist of macro-size particles.

For instance, it can be expressed that, contact surface relative to volume fraction for particles with 10 nm diameter, is 1000 times as much as particles with 10 μ m. Nanoparticles high contact surface in comparison with larger particles, not only causes to improve heat transfer ability but also increases stability ([Masuda et al., 1993](#)). [Xuan and Li \(2000\)](#) compared two kinds of nanofluid that one consisted in copper nanoparticles with 100 nm in diameter, and other consisted in copper nanoparticles with 10 nm in diameter. They showed that thermal conductivity of nanofluid which included smaller particles is higher than the one which is

made by larger particles. This is also confirmed with the recent works of [Li and Peterson \(2007\)](#). They showed that the thermal conductivity enhancement of the two nanofluids demonstrated a nonlinear relationship with respect to temperature, nanoparticles volume fraction, and nanoparticles size. In addition they found the importance of the nanoparticles size on the effective thermal conductivity.

Convective heat transfer with nanofluids can be modeled using the two-phase or single phase approach. The first provides the possibility of understanding the function of both the fluid phase and the solid particles in the heat transfer process. The second assumes that the fluid phase and particles are in thermal and hydrodynamic equilibrium. This approach is simpler and requires less computational time. Thus it has been used in several theoretical studies of convective heat transfer with nanofluids ([Maiga et al., 2004](#); [Khanafer et al., 2003](#); [Koo and Kleinstreuer, 2005](#); [Akbari and Behzadmehr, 2007](#); [Akbarinia and Behzadmehr, 2007](#)). However, due to the fact that the effective properties of nanofluids are known precisely, the numerical predictions of this approach are, in general, not in good agreement with experimental results. In addition, [Ding and Wen \(2005\)](#) showed that the particle concentration could only be assumed uniform if the corresponding Peclet numbers is always less than 10. Therefore, the concerns in single phase modeling consist in selecting the proper effective properties for nanofluids and taking into account the chaotic movement of ultra fine particles. To partially overcome this difficulty, some researches (for instance, [Xuan and Li, 2003](#); [Xuan and Roetzel, 2000](#)) have used the dispersion model which takes into account the improvement of heat transfer due to the random movement of particles in the main flow.

Due to several factors such as gravity, friction between the fluid and solid particles and Brownian forces, the phenomena of Brownian diffusion, sedimentation, and dispersion may coexist in the main flow of a nanofluid. This means that the slip velocity between the fluid and particles may not be zero ([Xuan and Li, 2003](#)); therefore it seems that the two-phase approach could better model nanofluid behaviors. Recently [Behzadmehr et al. \(2007\)](#) studied the turbulent forced convection of a nanofluid in a circular tube by using a two-phase approach. Their comparison with the experimental results showed that the two-phase mixture model is more precise than the single phase model. Therefore, [Mirmasoumi and Behzadmehr \(in press\)](#) studied the laminar mixed convection of a nanofluid in a horizontal tube using two-phase mixture model and showed the effects of particles volume fractions on the nanofluid thermal and hydrodynamic parameters.

Mixed convection in horizontal tubes at macro-size has been interested by many industries. Therefore, it has been studied extensively (for instance [Mori et al., 1966](#); [Petukhov et al., 1969](#); [Cheng and Yuen, 1985](#); [Barozzi et al., 1998](#); [Ciampi et al., 1986](#); [Zhang, 1992](#); [Hwang and Lai, 1994](#)). Heat transfer enhances in such a condition because of secondary flow that is generated by the buoyancy force.

Buoyancy force significantly affects the flow field, for instance at the fully development region, the maximum axial velocity does not appear at the tube centerline and radial variation of the temperature becomes important.

Following to our recent work ([Mirmasoumi and Behzadmehr, in press](#)), the present paper is investigated the effects of the nanoparticles' size on the thermal and hydrodynamic parameters of a laminar mixed convection. Therefore, for a given nanoparticles volume fraction, the effects of nanoparticles mean diameter, are presented over wide range of $Re-Gr$. In addition, the nanoparticles distributions at the tube cross section are shown and discussed.

2. Mathematical formulation

2.1. Mixture model

The mixture model, based on a single fluid two-phase approach, is employed in the simulation by assuming that the coupling between phases is strong and particles closely follow the flow. The two phases are assumed to be interpenetrating, meaning that each phase has its own velocity vector field, and within any control volume there is a volume fraction of primary phase and also a volume fraction of the secondary phase. Instead of utilizing the governing equations of each separately, the continuity, momentum and energy equations for the mixture are employed. A nanofluid composed of water and Al_2O_3 nanoparticles flowing in a long tube with uniform heating at the wall boundary is considered. The physical properties of the fluid are assumed constant except for the density in the body force, which varies linearly with the temperature (Boussinesq's hypothesis). Dissipation and pressure work are neglected. Therefore, the dimensional equations for steady state mean conditions are

Continuity equation:

$$\nabla \cdot (\rho_{eff} V_m) = 0 \quad (1)$$

Momentum equation:

$$\begin{aligned} \nabla \cdot (\rho_{eff,0} V_m V_m) = -\nabla P + \nabla \cdot [\tau] - \rho_{eff,0} \beta_{eff} (T - T_0) g \\ + \nabla \cdot \left(\sum_{k=1}^n \phi_k \rho_k V_{dr,k} V_{dr,k} \right) \end{aligned} \quad (2)$$

Energy equation:

$$\nabla \cdot \left[\sum_{k=1}^n (\rho_k c_k) \phi_k V_k T \right] = \nabla \cdot (k_{eff} \nabla T) \quad (3)$$

Volume fraction:

$$\nabla \cdot (\phi_p \rho_p V_m) = -\nabla \cdot (\phi_p \rho_p V_{dr,p}) \quad (4)$$

where

$$V_m = \frac{\sum_{k=1}^n \phi_k \rho_k V_k}{\rho_{eff}} \quad (5)$$

$$\tau = \mu_{eff} \nabla V_m \quad (6)$$

are the mean velocity and shear, respectively, and ϕ is the volume fraction of phase k .

In Eq. (2), $V_{dr,k}$ is the drift velocity for the secondary phase k , i.e. the nanoparticles in the present study.

$$V_{dr,k} = V_k - V_m \quad (7)$$

The slip velocity (relative velocity) is defined as the velocity of a secondary phase (p) relative to the velocity of the primary phase (f):

$$V_{pf} = V_p - V_f \quad (8)$$

The drift velocity is related to the relative velocity:

$$V_{dr,p} = V_{pf} - \sum_{k=1}^n \frac{\Phi_k \rho_k}{\rho_m} V_k \quad (9)$$

The relative velocity is determined from Eq. (10) proposed by Manninen et al. (1996) while Eq. (11) by Schiller and Naumann (1935) is used to calculate the drag function f_{drag} .

$$V_{pf} = \frac{\rho_p d_p^2}{18 \mu_f f_{drag}} \frac{(\rho_p - \rho_m)}{\rho_p} a \quad (10)$$

$$f_{drag} = \begin{cases} 1 + 0.15 Re_p^{0.687} & Re_p \leq 1000 \\ 0.0183 Re_p & Re_p > 1000 \end{cases} \quad (11)$$

The acceleration (a) in Eq. (10) is

$$a = g - (V_m \cdot \nabla) V_m \quad (12)$$

It should be mentioned that other correlations are also found in the literature for calculating the drag coefficient for instance (Ossen, 1913; Proudman and Pearson, 1957; Clift and Gauvin, 1970). Ossen (1913) developed a correlation which is adequate for $Re_p < 0.5$. Proudman and Pearson (1957) presented a higher order approximate solution which is reasonable up to $Re_p = 4$. A more accurate expression is given by Clift and Gauvin (1970) for $Re_p < 2 \times 10^5$. While the Schiller and Naumann (1935) drag expression is quite simple and accurate for $Re_p < 800$.

These correlations for calculating drag force were not developed for the nano-size particles. However, since Re_p is very low and the flow regime is considered laminar, we assume, it is reasonable to use such a correlation in the absence of a particular correlation for the nano-size particles.

The physical properties in the above equation are

Effective density:

$$\rho_{eff} = (1 - \phi) \rho_f + \phi \rho_p \quad (13)$$

Chon et al. (2005) correlation which considers the Brownian motion and nanoparticles mean diameter has been used for calculating the effective thermal conductivity

$$\frac{K_{eff}}{K_f} = 1 + 64.7 \times \phi^{0.7460} \left(\frac{d_f}{d_p} \right)^{0.3690} \left(\frac{K_s}{K_f} \right)^{0.7476} \times Pr^{0.9955} \times Re^{1.2321} \quad (14)$$

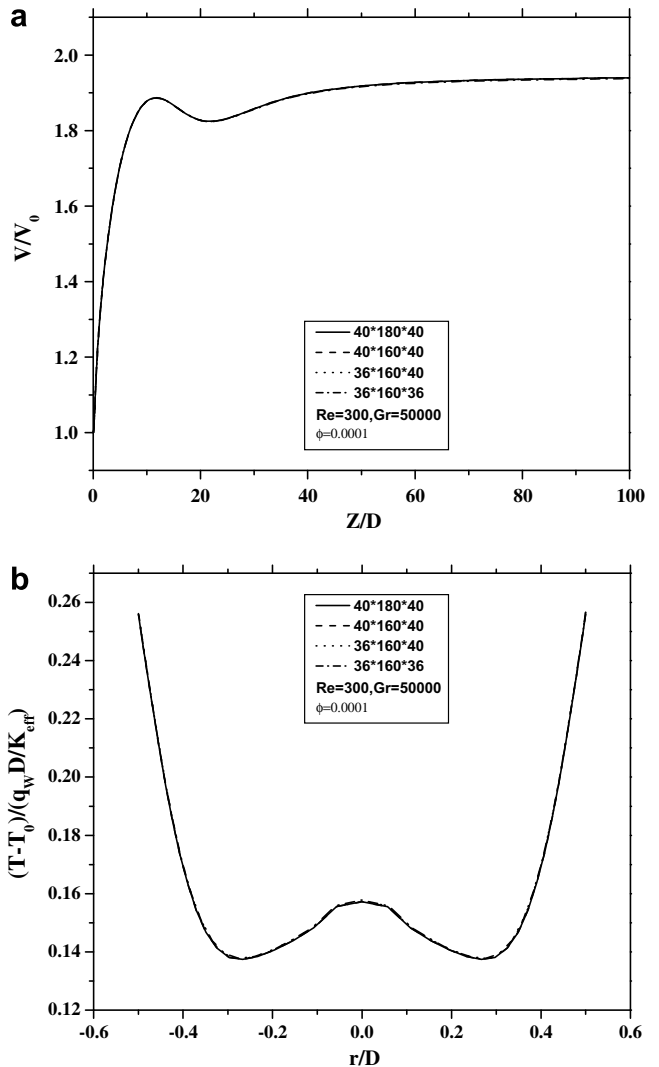


Fig. 1. Grid independence test (a) centerline axial velocity, (b) fully developed temperature.

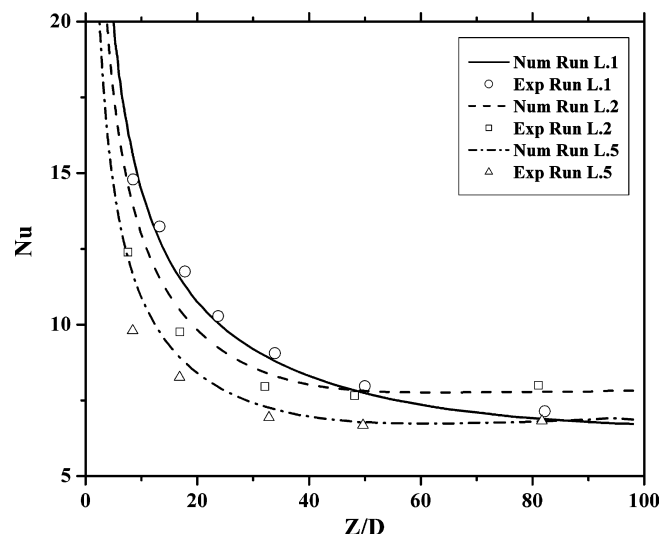


Fig. 2. Comparison of the axial evolution of Nu in a horizontal tube with the corresponding experimental results of Cheng and Yuen (1985).

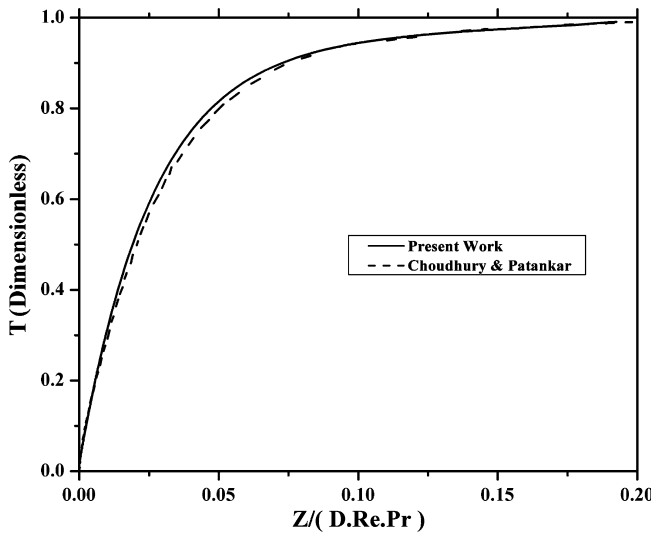


Fig. 3. Comparison of dimensionless temperature with the numerical results of Choudhury and Patankar (1988).

where Pr and Re in Eq. (14) are defined as

$$Pr = \frac{\mu}{\rho_{BF}\alpha} \quad (15)$$

$$Re = \frac{\rho_{BF}K_b T}{3\pi\mu^2 l_{BF}} \quad (16)$$

l_{BF} is the mean free path of water, K_b is the Boltzman constant (1.3807×10^{-23} J/K) and μ is calculated by the following equation:

$$\mu = A \times 10^{\frac{B}{T-C}}, \quad A = 2.414e-5, \quad B = 247, \quad C = 140 \quad (17)$$

Effective viscosity of water– Al_2O_3 nanofluid (Maiga et al., 2004):

$$\mu_{\text{eff}} = (123\phi^2 + 7.3\phi + 1)\mu_f \quad (18)$$

This was presented for water– Al_2O_3 nanofluid based on available experimental results in the literature.

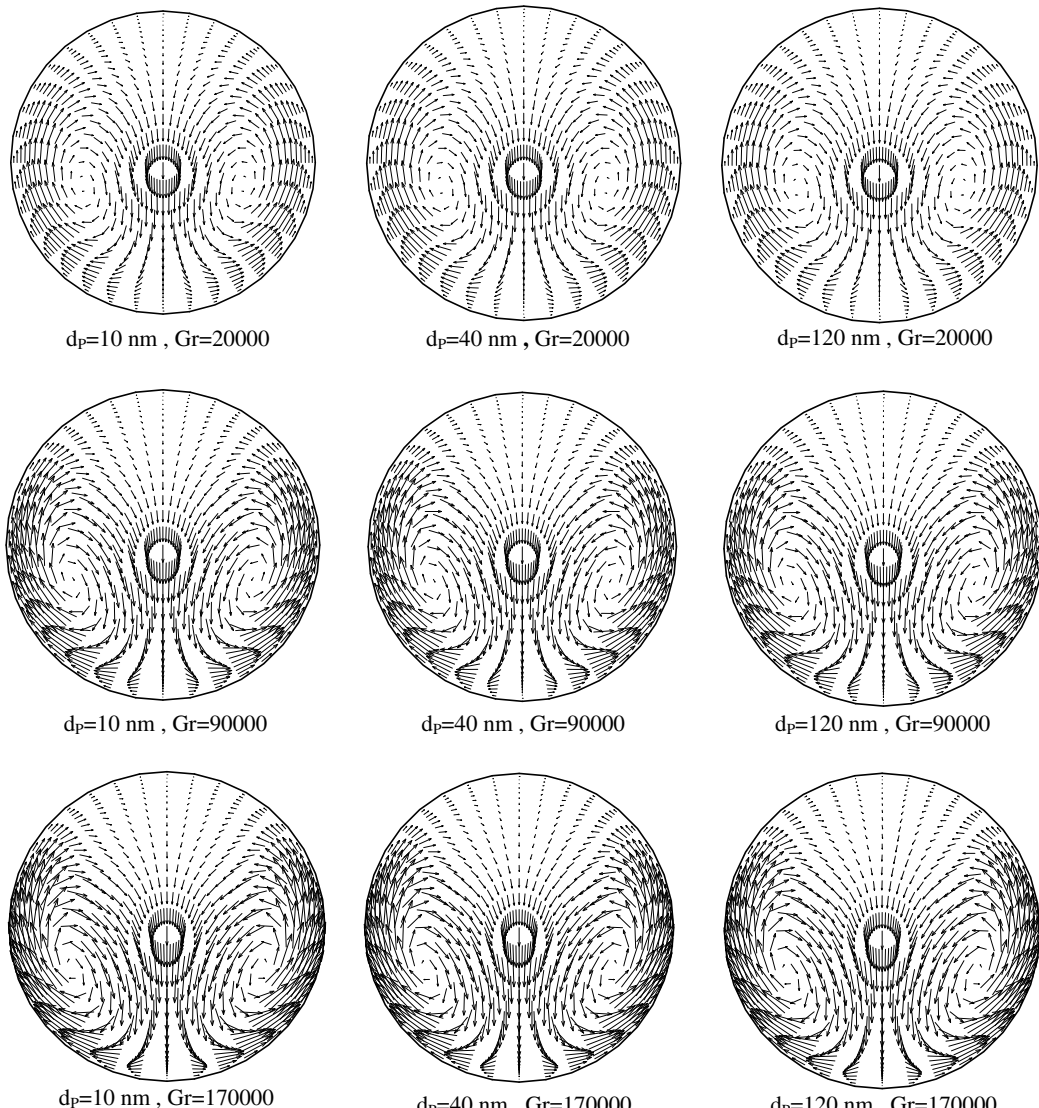


Fig. 4. Vectors of secondary flow for different Ri (or Gr) and d_p at $Re = 300$.

Thermal expansion coefficient (Khanafer et al., 2003):

$$\beta_{\text{eff}} = \left[\frac{1}{1 + \frac{(1-\phi)\rho_f}{\phi\rho_s} \beta_s} + \frac{1}{1 + \frac{\phi\rho_s}{(1-\phi)\rho_f} \beta_f} \right] \times \beta_f \quad (19)$$

2.2. Boundary condition

This set of nonlinear elliptical governing equation has been solved subject to the following boundary conditions:

– At the tube inlet ($Z=0$):

$$V_{mz} = V_0, \quad V_{m\theta} = V_{mr} = 0, \quad T = T_0 \quad (20)$$

– At the fluid–solid interface ($r = D/2$):

$$V_{mr} = V_{m\theta} = V_{mz} = 0 \quad \text{and} \quad -K \frac{\partial T}{\partial r} = q''_w \quad (21)$$

– At the tube outlet: the diffusion flux in the direction normal to the exit plan is assumed to be zero for all variables and an overall mass balance correction is also applied.

2.3. Numerical method and validation

This set of coupled nonlinear differential equation was discretized with the control volume technique. For the convective and diffusive terms a second order upwind method was used while the SIMPLEC procedure was introduced for the velocity–pressure coupling. The discretization grid is uniform in the circumferential direction and non-uniform in the other two directions. It is finer near the tube entrance and near the wall where the velocity and temperature gradients are large. Several different grid distributions have been tested to ensure that the calculated results are grid independent. The selected grid for the present calculations consisted of 160, 36 and 36 nodes, respectively, in the axial, radial and circumferential directions. As shown in Fig. 1a and b, increasing the grid numbers does not significantly change centerline axial velocity and also the fluid temperature, respectively, along the tube length and at the fully developed region. Other axial and radial profiles were also verified to be sure the results are grid independent.

In order to demonstrate the validity and also precision of the model and numerical procedure, comparisons with the available experimental and numerical simulation have been done. Fig. 2 shows the comparison of the calculated results with the experimental results of Barozzi et al. (1998) in a horizontal tube. Axial evolution of the Nusselt number at different Rayleigh numbers was compared. Good agreement between the results is seen. Another comparison has also been performed with the numerical results obtained by Choudhury and Patankar (1988). Axial evolution of the dimensionless temperature (peripherally averaged temperature) along the tube length is in good

concordance with the present results (see Fig. 3). It should be mentioned that our numerical results are obtained using the two-phase mixture model considering a very small volume fraction for the solid particles. Therefore the numerical procedure is reliable and can predict developing mixed convection flow in a horizontal tube.

3. Results and discussion

Numerical simulations have been done over a wide range of Re , Gr , particle volume fraction and particle diameter. However, the results are presented at $Re = 300$ for three different Grashof numbers (corresponding to the

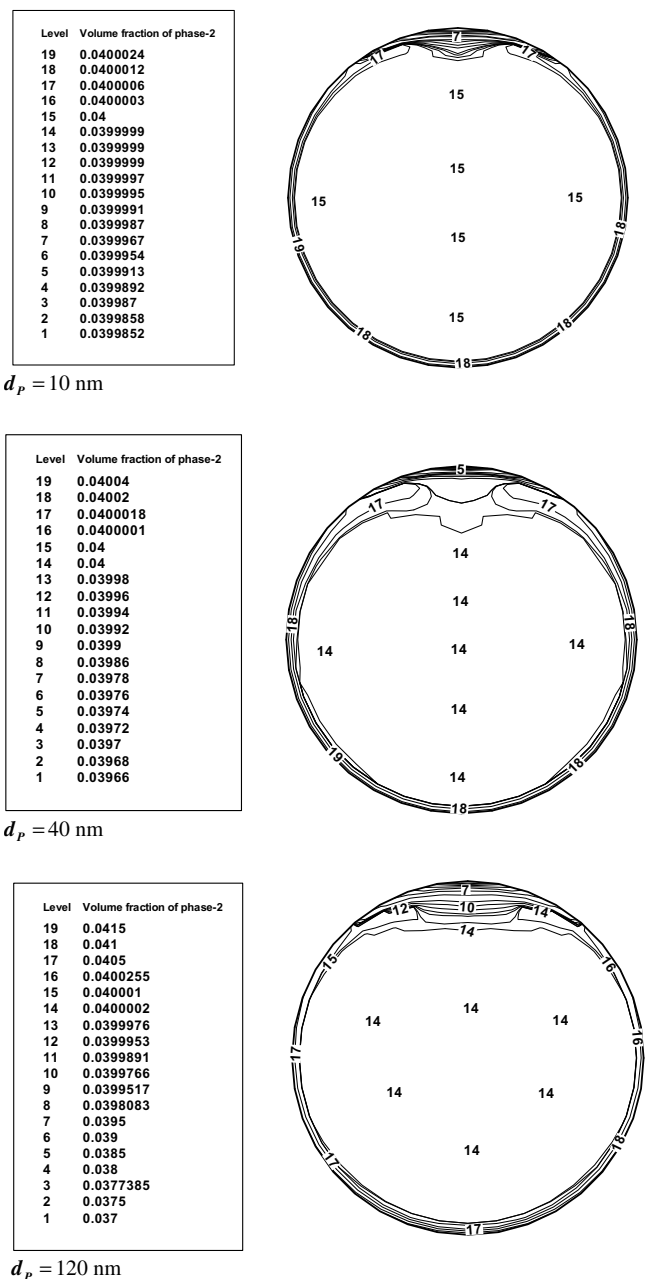


Fig. 5. Contours of nanoparticles distribution at fully developed region, $Re = 300$, $\phi = 4\%$ and $Gr = 2 \times 10^4$.

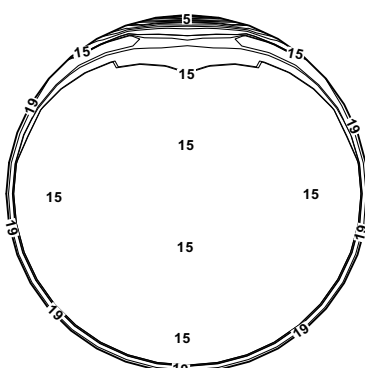
Richardson numbers equal to 0.22, 1 and 1.9), and for three particle mean diameter (spherical shape) with 4% particles volume fraction. Maximum Grashof number (or wall heat flux) at each Reynolds number are limited by the value of increasing the bulk temperature. This value respects the suggested criteria for validation of the Boussinesq approximation (Nesreddine et al., 1997).

For a given Re and a nanoparticles volume fraction ($\phi = 4\%$) and three different values of the Al_2O_3 particles diameter (10, 40 and 120 nm), vectors of secondary flow at fully developed region are presented in Fig. 4 for three Grashof numbers ($Ri = 0.22, 1$ and 1.9). Mean flow rises

to the top of the tube and falls down slowly toward the centre (through the vertical plane) because of the buoyancy force. Therefore, a secondary flow pattern appears at the tube cross section and creates a circular cell. The position of the cell depends on the buoyancy force and the inertia of the secondary flow at the vertical plane (symmetry plane).

It is seen that the nanoparticles mean diameter does not have significant effect on the secondary flow. However, this secondary flow could strongly affect the distribution of the nanoparticles as shown in Figs. 5–7. It should be mentioned

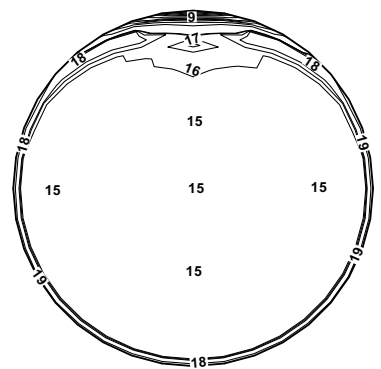
Level	Volume fraction of phase-2
19	0.0400008
18	0.0400002
17	0.0400002
16	0.04
15	0.04
14	0.039999
13	0.039998
12	0.039997
11	0.039995
10	0.039994
9	0.039992
8	0.039991
7	0.03999
6	0.039988
5	0.039987
4	0.039986
3	0.039984
2	0.039983
1	0.039982



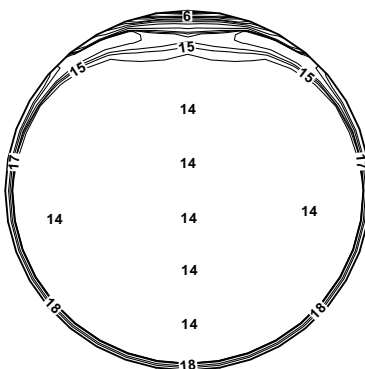
$d_p = 10 \text{ nm}$

Level	Volume fraction of phase-2
19	0.0400005
18	0.0400002
17	0.0400001
16	0.04
15	0.04
14	0.039999
13	0.039998
12	0.039997
11	0.039996
10	0.039995
9	0.039993
8	0.039991
7	0.03999
6	0.039989
5	0.039988
4	0.039987
3	0.039986
2	0.039985
1	0.039984

$d_p = 10 \text{ nm}$



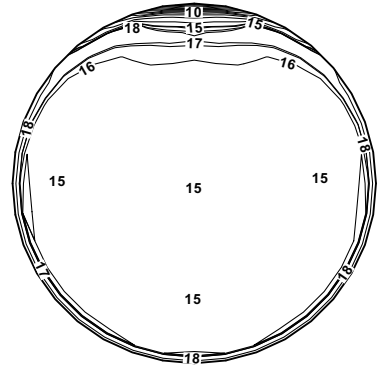
Level	Volume fraction of phase-2
19	0.0400127
18	0.0400087
17	0.0400035
16	0.040002
15	0.0400014
14	0.0400006
13	0.0399963
12	0.03998
11	0.03996
10	0.03994
9	0.03992
8	0.03988
7	0.03986
6	0.03984
5	0.03978
4	0.03976
3	0.03974
2	0.03972
1	0.0397



$d_p = 40 \text{ nm}$

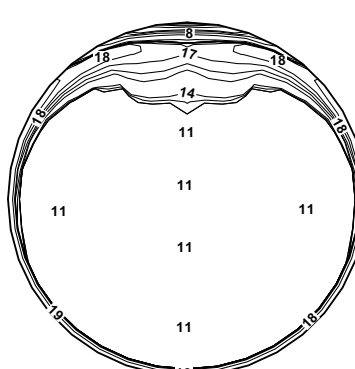
Level	Volume fraction of phase-2
19	0.0400087
18	0.0400021
17	0.0400018
16	0.0400005
15	0.04
14	0.0399948
13	0.03998
12	0.03996
11	0.03994
10	0.03992
9	0.0399
8	0.03988
7	0.03986
6	0.03984
5	0.03982
4	0.0398
3	0.03978
2	0.03976
1	0.03974

$d_p = 40 \text{ nm}$



Level	Volume fraction of phase-2
19	0.0400886
18	0.0400316
17	0.0400141
16	0.0400055
15	0.0400027
14	0.0400003
13	0.0400002
12	0.0400001
11	0.0400001
10	0.03997
9	0.0398
8	0.0396
7	0.0394
6	0.0392
5	0.0384
4	0.038
3	0.0378
2	0.0374
1	0.0372

$d_p = 120 \text{ nm}$



Level	Volume fraction of phase-2
19	0.0400689
18	0.0400269
17	0.0400209
16	0.040018
15	0.0400039
14	0.0400001
13	0.0400001
12	0.04
11	0.0399451
10	0.0398
9	0.0396
8	0.0394
7	0.039
6	0.0388
5	0.0384
4	0.0382
3	0.0378
2	0.0376
1	0.0374

$d_p = 120 \text{ nm}$

Fig. 6. Contours of nanoparticles distribution at fully developed region, $Re = 300$, $\phi = 4\%$ and $Gr = 9 \times 10^4$.

Fig. 7. Contours of nanoparticles distribution at fully developed region, $Re = 300$, $\phi = 4\%$ and $Gr = 1.7 \times 10^5$.

that the correlations which have been used to calculate the particles relative velocity are those that were developed for micro and milli size particles. It could qualitatively show particles distribution because of different forces in the tube. Figs. 5–7 show the contours of the nanoparticles distribution at the fully developed region for $Re = 300$, $\phi = 4\%$ and three different nanoparticles mean diameter ($d_p = 10 \text{ nm}$, 40 nm , 120 nm) at the three Grashof numbers. In general, the nanoparticles concentration is higher at the wall vicinity for which the viscous forces are important. At the proximity of top wall of the tube, the nanoparticles concentration decreases as result of the secondary flow at the tube cross section. For the particles with small mean diameter, this variation is not significant and thus uniform particles distribution could be considered. While, increasing the nanoparticles mean diameter, non-uniformity on the particles distribution becomes more important. Increasing the Grashof number intensifies non-uniformity of the parti-

cles distributions and could also affect the particles distribution even for a nanofluid with a small mean diameter.

As they are shown, for the particles with very small diameter ($d_p = 10 \text{ nm}$ and 40 nm) and with relatively low Richardson number the particles distribution is fairly uniform and single phase approach could be well adopted. While increasing the nanoparticles mean diameter and/or Grashof numbers non-uniformity on the particles distribution becomes important and thus single phase approach could not well predicted the flow parameters. Many researches have been shown that the presence of nanoparticles could significantly increases the heat transfer coefficient. On the other hand, the effect of particles size on the heat transfer phenomena has not been studied so much. Fig. 8 shows the effect of mean diameter of the nanoparticles on the convective heat transfer coefficient along the tube length for a given particles volume fraction ($\phi = 4\%$) at two different Grashof numbers. In all cases, the

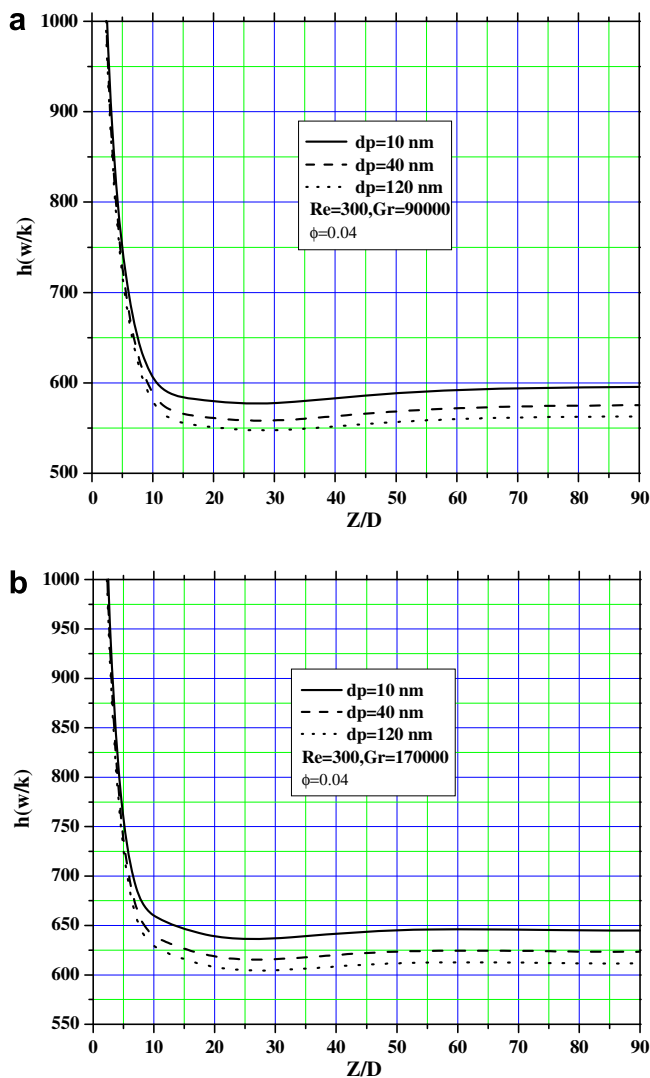


Fig. 8. Axial evolution of peripherally averaged convective heat transfer coefficient along the tube length.

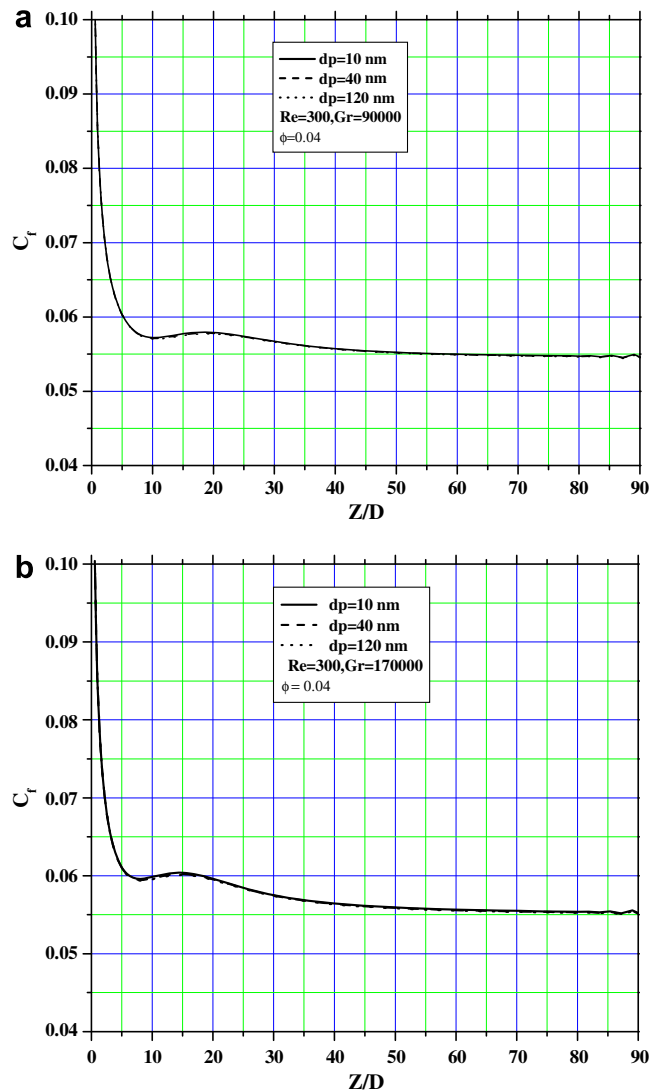


Fig. 9. Axial evolutions of peripherally averaged skin friction coefficient along the tube length.

convective heat transfer coefficient decreases at the tube entrance and then goes monotonically to its asymptotic value further downstream. Convective heat transfer coefficient increases with decreasing the nanoparticles mean diameter. This tendency is also seen for different particles volume fraction but not present. In spite of considerable heat transfer augmentation, skin friction coefficient is not significantly affected by the nanoparticles mean diameter. This is shown in Fig. 9.

4. Conclusion

Fully developed laminar mixed convection of a nanofluid consisting of water and Al_2O_3 has been studied numerically. Two-phase mixture model has been used to investigate numerically the effect of nanoparticles mean diameter on the hydrodynamic and thermal parameters. Using particles with smaller diameter increases the uniformity of the particles distribution at the tube cross section. While, increasing nanoparticles mean diameter and/or Grashof numbers could result non-uniform distribution for which the single phase approach no longer would be precise. It is shown that the convective heat transfer coefficient could be significantly increased by using particles with smaller mean diameter while the skin friction coefficient does not notably change.

References

Akbari, M., Behzadmehr, A., 2007. Developing laminar mixed convection of a nanofluid in a horizontal tube with uniform heat flux. *Int. J. Numer. Method Heat Fluid Flow* 17 (6), 566–586.

Akbarinia, A., Behzadmehr, A., 2007. Numerical study of laminar mixed convection of a nanofluid in a horizontal curved tube. *Appl. Therm. Eng.* 27, 1327–1337.

Barozzi, G.S., Zanchini, E., Mariotti, M., 1998. Experimental investigation of combined forced and free convection in horizontal and inclined tubes. *Meccanica* 20, 18–27.

Behzadmehr, A., Saffar-Avval, M., Galanis, N., 2007. Prediction of turbulent forced convection of a nanofluid in a tube with uniform heat flux using a two-phase approach. *Int. J. Heat Fluid Flow* 28, 211–219.

Cheng, K.C., Yuen, F.P., 1985. Flow visualization studies on secondary flow pattern for mixed convection in the thermal entrance region of isothermally heated inclined pipes. *ASME Heat Transfer Div.* 42, 121–130.

Choi, S.U.S., 1995. Enhancing thermal conductivity of fluid with nanoparticles, developments and applications of non-Newtonian flow, *ASME, FED 231/MD 66*, pp. 99–105.

Choi, S.U.S., Zhang, Z.G., Yu, W., Lockwood, F.E., Grulke, E.A., 2001. Anomalous thermal conductivity enhancement in nanotube suspensions. *Appl. Phys. Lett.* 79, 2252–2254.

Chon, C.H., Kihm, K.D., Lee, S.P., Choi, S.U.S., 2005. Empirical correlation finding the role of temperature and particle size for nanofluid (Al_2O_3) thermal conductivity enhancement. *Appl. Phys. Lett.* 87, 1–3.

Choudhury, D., Patankar, S.V., 1988. Combined forced and free laminar convection in the entrance region of an inclined isothermal tube. *ASME J. Heat Transfer Trans.* 110, 901–909.

Ciampi, M., Faggiani, S., Grassi, W., Incropera, F.P., Tuoni, G., 1986. Experimental study of mixed convection in horizontal annuli for low Reynolds numbers. *Proc. Int. Heat Transfer Conf.* 3, 1413–1418.

Clift, R., Gauvin, W.H., 1970. The motion of particles in turbulent gas stream. *Proc. Chem. E.C.A.* 1, 14–24.

Ding, Y., Wen, D., 2005. Particle migration in a flow of nanoparticle suspensions. *Powder Technol.* 149, 84–92.

Estman, J.A., Choi, S.U.S., Li, S., Yu, W., Thomson, L.J., 2001. Anomalously increased effective thermal conductivities of ethylene glycol based nanofluid containing copper nanoparticles. *Appl. Phys. Lett.* 78, 718–720.

Hwang, G.J., Lai, H.C., 1994. Laminar convection heat transfer in a horizontal isothermal tube for high Reynolds numbers. *Int. J. Heat Mass Transfer* 37, 1631–1640.

Jang, S.P., Choi, S., 2004. Role of Brownian motion in the enhanced thermal conductivity of nanofluids. *Appl. Phys. Lett.* 84, 4316–4318.

Keblinski, P., Phillpot, S.R., Choi, S.U.S., Eastman, J.A., 2002. Mechanisms of heat flow in suspensions of nano-sized particles (nanofluid). *Int. J. Heat Mass Transfer* 45, 855–863.

Khanafer, K., Vafai, K., Lightstone, M., 2003. Buoyancy-driven heat transfer enhancement in a two dimensional enclosure utilizing nanofluids. *Int. J. Heat Mass Transfer* 46, 3639–3653.

Koo, J., Kleinstreuer, C., 2005. Laminar nanofluid flow in microheat-sinks. *Int. J. Heat Mass Transfer* 48, 2652–2661.

Lee, S., Choi, S.U.S., Li, S., Eastman, J.A., 1999. Measuring thermal conductivity of fluids containing oxide nanoparticles. *J. Heat Transfer* 121, 280–289.

Li, C.H., Peterson, G.P., 2007. The effect of particles size on the effective thermal conductivity of Al_2O_3 –water nanofluids. *J. Appl. Phys.* 101, 044312.

Maiga, S.E., Nguyen, C.T., Galanis, N., Roy, G., 2004. Heat transfer behaviors of nanofluids in a uniformly heated tube. *Super Lattices Microstruct.* 35, 543–557.

Manninen, M., Taivassalo, V., Kallio, S., 1996. On the mixture model for multiphase flow. *Technical Research Center of Finland, VTT Publications* 288, pp. 9–18.

Masuda, H., Ebata, A., Teramae, K., Hishinuma, N., 1993. Alteration of thermal conductivity and viscosity of liquid by dispersing ultra-fine particles (dispersions of Al_2O_3 , SiO_2 , and TiO_2 ultra-fine particles). *Netsu Bussei (Japan)* 4, 227–233.

Mirmasoumi, S., Behzadmehr, A., in Press. Numerical study of laminar mixed convection of a nanofluid in a horizontal tube using two-phase mixture model. *J. Appl. Therm. eng.*

Mori, Y., Futagami, K., Tokuda, S., Nakamura, M., 1966. Forced convective heat transfer in uniformly heated horizontal tubes, 1st report, Experimental study on the effect of buoyancy. *Int. J. Heat Mass Transfer* 9, 453–463.

Nesreddine, H., Galanis, N., Nguyen, C.T., 1997. Variable-property effects in laminar aiding and opposing mixed convection of air in vertical tubes. *Numer. Heat Transfer; Part A* 31, 53–69.

Ossen, C.W., 1913. Über den geltungsbereich der stokeschen widerstandsformel. *Ark. Mat. Astron. Fysik* 9.

Pak, B.C., Cho, Y.I., 1998. Hydrodynamic and heat transfer study of dispersed fluids with submicron metallic oxide particles. *Exp. Heat Transfer* 11, 151–170.

Petukhov, B.S., Polyakov, A.F., Strigin, B.S., 1969. Heat transfer in tubes with viscous – gravity flow. *Heat Transfer – Soviet Res.* 1, 24–31.

Proudman, I., Pearson, J.R.A., 1957. Expansions at small Reynolds number for the flow past a sphere and a cylinder. *J. Fluid Mech.* 2, 237–262.

Schiller, L., Naumann, A., 1935. A drag coefficient correlation. *Z. Ver. Deutsch. Ing.* 77, 318–320.

Wang, X., Xu, X., Choi, S.U.S., 1999. Thermal conductivity of nanoparticle-fluid mixture. *J. Thermophys. Heat Transfer* 13, 474–480.

Wen, D., Ding, Y., 2004. Experimental investigation into convective heat transfer of nanofluids at the entrance region under laminar flow conditions. *Int. J. Heat Mass Transfer* 47, 5181–5188.

Xuan, Y.M., Li, Q., 2000. Heat transfer enhancement of nanofluids. *Int. J. Heat Fluid Flow* 21, 58–64.

Xuan, Y.M., Li, Q., 2003. Investigation on convective heat transfer and flow features of nanofluids. *J. Heat Transfer* 125, 151–155.

Xuan, Y.M., Li, Q., Hu, W., 2003. Aggregation structure and thermal conductivity of nanofluids. *AICHE J.* 49, 1038–1043.

Xuan, Y.M., Roetzel, W., 2000. Conceptions for heat transfer correlation of nanofluids. *Int. J. Heat Mass Transfer* 43, 3701–3707.

Xue, Q.Z., 2003. Model for effective thermal conductivity of nanofluids. *Phys. Lett. A* 307, 313–317.

Zhang, X., Gu, H., Fujii, M., 2007. Effective thermal conductivity and thermal diffusivity of nanofluids containing spherical and cylindrical nanoparticles. *Exp. Therm. Fluid Sci.* 31, 593–599.

Zhang, C., 1992. Mixed convection inside horizontal tubes with nominally uniform heat flux. *AICHE Symp. Ser.* 88, 212–219.